International Journal of Modern Physics E
Vol. 25, No. 3 (2016) 1650023 (11 pages)

DOI: 10.1142/S0218301316500233

Breakup of ^{16}O nucleus onto C and He isotopes by protons at incident momentum of 3.25A GeV/c

Kosim Olimov*, Khusniddin K. Olimov*,†,‡,¶,
Sagdulla L. Lutpullaev*, Erkin Kh. Bazarov§, Alisher K. Olimov*,
Vladimir V. Lugovoi*, K. G. Gulamov* and Vadim Sh. Navotny*

*Physical Technical Institute of SPA Physics Sun,
of Uzbek Academy of Sciences, Tashkent, Uzbekistan

†Inha University in Tashkent, Tashkent, Uzbekistan

‡Department of Physics,
COMSATS Institute of Information Technology,
Islamabad, Pakistan

§Institute of Nuclear Physics, Tashkent, Uzbekistan

¶drolimov@gmail.com

Received 31 December 2015
Revised 15 February 2016
Accepted 16 February 2016
Published 9 March 2016

Phenomenological analysis of breakup of oxygen nuclei on fragments with charges two and six in collisions with protons at 3.25A GeV/c was conducted using the Monte Carlo (MC) model of isotropic phase space. For the first time, the contributions of mechanism of diffractive breakup of oxygen nucleus, and that of quasi elastic knocking out of one of the α clusters of oxygen nucleus by a proton target, into channel of formation of α particle and ^{12}C nucleus with conservation of recoil proton were determined in final state. The substantial role of α cluster structure of initial nucleus in processes of fragmentation of oxygen nuclei in peripheral interactions with protons was revealed in experiment.

Keywords: Fragmentation of nuclei; structure of nuclei; excitation of nuclei; formation of light nuclei.

PACS Number(s): 25.10.+s, 27.20.+n

1. Introduction

Investigation of fragmentation of light nuclei in peripheral collisions with nucleons and nuclei allows one to obtain unique information about initial structure of fragmenting nuclei and its interrelation with the yield and composition of the final reaction products. In recent years, International BECQUEREL collaboration conducted research of the cluster structures of light relativistic nuclei in peripheral

¶Corresponding author.

interactions with emulsion nuclei and obtained interesting results.[1–6] In particular, they showed experimentally that, in extremely peripheral interactions of light relativistic nuclei with emulsion nuclei, not only α cluster structure, but also clusters including light ^{2}H, ^{3}H, and ^{3}He nuclei in combination with ^{4}He nuclei may exist in light nuclei.[1–6] The composition of the cluster structure of light nuclei is determined by their type: even–even, odd–odd, even–odd, or odd–even nucleus.[1–6]

The new experimental data on dependencies of the mean multiplicities and kinematical characteristics of ^{4}He nuclei, formed in ^{16}Op collisions at $3.25A\,\mathrm{GeV}/c$, on degree of excitation of the fragmenting nucleus were presented in our recent work.[7] It was shown that an initial (α cluster) structure of oxygen nucleus was retained at small excitation levels. It was established that the kinematical characteristics of ^{1}H, ^{2}H, ^{3}H and ^{3}He fragments did not depend on availability or absence of α particles in a collision event, which indicated the independence of mechanisms of formation of such fragments and ^{4}He nuclei.[7]

While studying the breakup of oxygen nuclei in interactions with protons at $3.25A\,\mathrm{GeV}/c$ on multicharged fragments (with $Z \geq 2$) with their total charge equal to that of initial oxygen nucleus, it was observed that from the experimentally observable three channels ((26), (224) and (2222)) with the total charge of fragments equal to eight, only in two of topologies ((26) and (2222)) all the nucleons of the initial oxygen nucleus were conserved. Here, the single digits denote the charges of multicharged fragments and their number is the total number of such fragments in a collision event. Among these topologies, the maximal yield cross-section belongs to topology $(26) - 10.14\,\mathrm{mb}$, and the minimal yield cross-section is observed for topology $(224) - 0.93 \pm 0.18\,\mathrm{mb}$.[8]

In Ref. 9, we studied the characteristics of three-prong events of topology (26) with conservation of a recoil proton to search and analyze diffractive breakup of oxygen nucleus into α particle and carbon-12 nucleus. Based on analysis of shape of spectra on difference of azimuthal angles of α particle and recoil proton, it was observed that a breakup of oxygen nucleus on α particle and carbon-12 nucleus could proceed via two ways: (1) direct breakup resulting from excitation of oxygen nucleus as a whole, i.e., diffractive mechanism; (2) breakup of oxygen nucleus resulting from quasi elastic knocking out of one out of four α clusters of oxygen nucleus by a recoil proton. The present paper continues works[7–9] and is devoted to detailed analysis of topology (26), and determination of contribution of the above mentioned mechanisms of oxygen nucleus breakup into α particle and carbon-12 nucleus.

2. Analysis and Results

The experimental data were obtained using 1 m hydrogen bubble chamber of the Laboratory of High Energies (LHEs) of Joint Institute for Nuclear Research (JINR), irradiated by oxygen nuclei with momenta $3.25A\,\mathrm{GeV}/c$, accelerated at Dubna synchrophasotron,[10] and consist of 8712 fully measured inelastic ^{16}Op collision events. For identification of mass of fragments, the following momentum intervals

in laboratory frame were introduced. Singly charged fragments with $1.75\,\mathrm{GeV}/c < p \leq 4.75\,\mathrm{GeV}/c$ were considered to be protons, those with $4.75\,\mathrm{GeV}/c < p \leq 7.75\,\mathrm{GeV}/c$, and $p > 7.75\,\mathrm{GeV}/c$ were taken to be ^{2}H and ^{3}H nuclei, respectively. Doubly charged fragments with $p \leq 10.75\,\mathrm{GeV}/c$ and $p > 10.75\,\mathrm{GeV}/c$ were considered to be ^{3}He and ^{4}He nuclei, respectively. Fragments having the charge of six and belonging to momentum intervals $p \leq 34.1\,\mathrm{GeV}/c$, $34.1\,\mathrm{GeV}/c < p \leq 37.35\,\mathrm{GeV}/c$, $37.35\ \mathrm{GeV}/c < p \leq 40.6\,\mathrm{GeV}/c$, and $p > 40.6\,\mathrm{GeV}/c$ were taken to be ^{10}C, ^{11}C, ^{12}C and ^{13}C nuclei, respectively. At such a selection, the admixture of neighboring isotopes among selected fragments, due to overlap of their momentum distributions, does not exceed 5%.[10] Such separation of fragments by their charge and mass allows one to determine the multiplicity of bound neutrons in multicharged fragments in each individual collision event. Since the number of bound protons in the studied topology (26) equals to eight, it is also possible to determine the multiplicity of unbound neutrons using the law of conservation of electrical and baryon charges.

Let us consider distribution of events on the number of charged particles (including multicharged fragments) in topology (26) depending on availability or absence of recoil proton in an event. In Table 1, the number of events of topology (26) depending on the number of charged particles (n_z) with (or without) recoil proton (n_{pr}) is presented.

As seen from Table 1, the main fraction (88%) of topology (26) consists of events with three charged (three-prong events) particles in final state, and 83% of events among these are those with recoil protons. On the whole, the fraction of events with recoil proton for topology (26) is 82%, and 18% are events without recoil proton. As observed from Table 1, there is not even a single event with recoil proton among seven-prong events, i.e., those having five charged pions — three positively charged and two negatively charged ones. Apparently, due to quite low incident energy, production of five charged pions in a collision event is very unlikely. In seven–prong events with recoil proton, formation of proton fragment is not observed.

Analysis of composition of singly charged fragments in topology (26) showed an absence of events with formation of ^{2}H or ^{3}H nuclei in final state. Since in topology (26) formation of the singly charged fragment — proton, deuteron, or tritium is connected with the processes of inelastic charge exchange of projectile neutron ($n \to p + \pi^{-}$), or transfer of a charge of target proton to one of the neutrons

Table 1. Distribution of events on the number of charged particles from topology (26) depending on availability or absence of recoil proton (n_{pr}) in an event.

	n_{z}			
n_{pr}	3	5	7	The total number
0	35	8	—	43
1	173	18	2	193
All	208	26	2	236

Table 2. The mean multiplicities per event of charged pions ($\langle n(\pi^-)\rangle, \langle n(\pi^+)\rangle$), recoil protons ($\langle n_{\rm pr}\rangle$) and proton fragments ($\langle n_{\rm p}\rangle$) in events of topology (26).

$\langle n(\pi^-)\rangle$	$\langle n(\pi^+)\rangle$	$\langle n_{\rm pr}\rangle$	$\langle n_{\rm p}\rangle$
0.13 ± 0.02	0.15 ± 0.02	0.82 ± 0.05	0.16 ± 0.02

of oxygen nucleus ($np \to pn$) or to multinucleon system — remnant nucleus, this confirms the early observation[11] that the charge of target proton practically does not participate in formation of multinucleon fragments.

Let us consider the mean multiplicities per event of charged pions, recoil protons, and proton fragments in events of topology (26), given in Table 2.

As observed from Table 2, the recoil proton is conserved, as mentioned above, in majority of events of topology (26). The mean multiplicities of both types of charged pions and proton fragments coincide within statistical uncertainties. Due to conservation of electrical charge, proton fragment is absent in three-prong events with recoil proton. In experiment, formation of proton fragments is observed in events with three charged particles without recoil proton, and with five charged particles in final state. As mentioned above, the experimentally observed proton fragments in topology (26) can be formed due to inelastic charge exchange of a projectile neutron ($n \to p + \pi^-$) or as a result of transfer of a charge of target proton to one of the neutrons of oxygen nucleus ($np \to pn$). Analysis showed that the contributions of the first and second processes to formation of proton fragments coincided within statistical uncertainties, being equal to $56 \pm 12\%$ and $44 \pm 12\%$, respectively.

Let us turn to analysis of isotope composition of fragments with charges two and six in topology (26), presented in Table 3.

As seen from Table 3, the highest probability of yield among doubly charged fragments and fragments with the charge of six belongs to α particles and ^{12}C nuclei, respectively. Among isotopes of fragments with charges two and six, the lowest probability of yield is observed for ^{13}C isotope accompanied by ^{3}He isotope. As the events of topology (26) proceed mainly at peripheral interactions (at low excitation energies), initial α cluster structure of oxygen nucleus is conserved with the highest probability. At knocking out of one of the α clusters of oxygen nucleus by a target proton, ^{12}C nucleus can be formed from the remaining three α clusters provided that the excitation of a remnant nucleus is sufficiently small. Therefore, the highest yield in experiment should be observed for events with formation of

Table 3. Isotope composition of fragments with charges two and six in topology (26).

Isotopes of helium nuclei		Isotopes of carbon nuclei			
^{3}He	^{4}He	^{10}C	^{11}C	^{12}C	^{13}C
0.16 ± 0.03	0.84 ± 0.06	0.15 ± 0.03	0.20 ± 0.04	0.61 ± 0.05	0.04 ± 0.01

Table 4. Distributions on pair isotope composition of fragments with charges two and six in topology (26).

Pair isotope composition of fragments with charges two and six						
^{3}He^{10}C	^{3}He^{11}C	^{3}He^{12}C	^{3}He^{13}C	^{4}He^{10}C	^{4}He^{11}C	^{4}He^{12}C
9	12	9	8	26	36	136

a pair isotope ^{4}He^{12}C and recoil proton. To confirm this statement, let consider distributions of events on pair isotope composition among fragments with charges two and six in topology (26). Distributions on pair isotope composition among fragments with charges two and six in topology (26) are presented in Table 4.

As seen from Table 4, the largest yield among pair isotopes of fragments with charges two and six is observed for pair isotope ^{4}He^{12}C, which points out the α cluster structure of oxygen nucleus. Due to conservation of electrical and baryon charges, the yield of pair isotope ^{4}He^{12}C is observed in three-prong events with conservation of recoil proton mainly. Using distributions on pair isotope composition of fragments with charges two and six, we determined the average number of nucleons in multicharged fragments, which proved to be 15.37 ± 0.06. Then using this value and the mean multiplicity of proton fragments, based on conservation of baryon number, we determined the mean multiplicity of neutron fragments, which proved to be 0.47 ± 0.04. Thus the total mean multiplicity of the conserved neutrons of projectile nucleus in topology (26) proved to be 7.84 ± 0.06, and that of protons -8.16 ± 0.06.

Let us turn now to analysis of three-prong events with recoil proton (Table 5). As seen from Table 5, in 112 out of 173 three-prong events with recoil proton (which makes up about 2/3 of the total number of events), the joint formation of α particle and ^{12}C nucleus is observed. Due to conservation of electrical and baryon charges in three-prong events with recoil proton, the joint formation of α particle and ^{13}C nucleus is forbidden, which is confirmed in experiment.

Let us consider the emission angle distribution of recoil protons in laboratory frame for three-prong events with yield of a pair isotope ^{4}He^{12}C (see Fig. 1) in reaction

$$^{16}\mathrm{O} + p \rightarrow {}^4\mathrm{He} + {}^{12}\mathrm{C} + p. \quad (1)$$

As seen from Fig. 1, the angular spectrum of recoil protons at $\theta < 70^\circ$ is practically isotropic and not significant, whereas at $\theta \geq 70^\circ$ abrupt rise of the

Table 5. Distributions of events on pair isotope composition of fragments with charges two and six in three-prong events with recoil proton from topology (26).

Pair isotope composition of fragments with charges two and six							
^{3}He^{10}C	^{3}He^{11}C	^{3}He^{12}C	^{3}He^{13}C	^{4}He^{10}C	^{4}He^{11}C	^{4}He^{12}C	^{4}He^{13}C
3	7	6	3	16	26	112	—

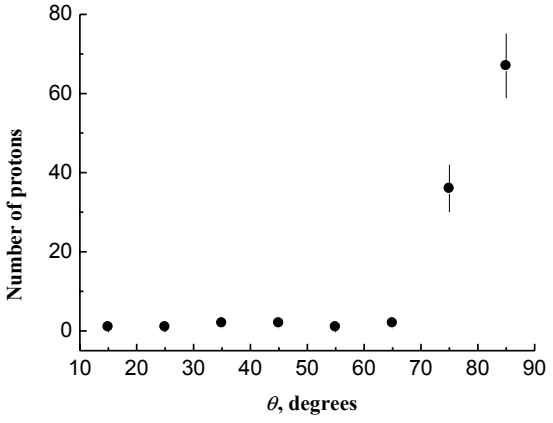

Fig. 1. Emission angle distribution of recoil protons for reaction in (1).

spectrum with maximum at $\theta = 85^\circ$ is observed. Such behavior of the angular spectrum of recoil protons suggests the different mechanisms of their formation. Recoil protons with emission angles $\theta < 70^\circ$ can be referred to those knocked out inelastically, and those with $\theta \geq 70^\circ$ to recoil protons knocked out quasi elastically by oxygen nucleus or its part, for example, by its α cluster. Thus the part of events having recoil proton with emission angle $\theta \geq 70^\circ$ can be classified as the events of diffractive breakup of oxygen nucleus. For more correct separation of such events, we considered the momentum spectrum of recoil protons with emission angle $\theta \geq 70^\circ$. After such angular constraint on recoil protons, there remained 103 collision events.

The momentum distribution of recoil protons with emission angle $\theta \geq 70^\circ$ for reaction in (1) is shown in Fig. 2. It is seen that the momentum spectrum of recoil protons demonstrates a single mode shape with the maximum at $p \approx 230\,\mathrm{MeV}/c$

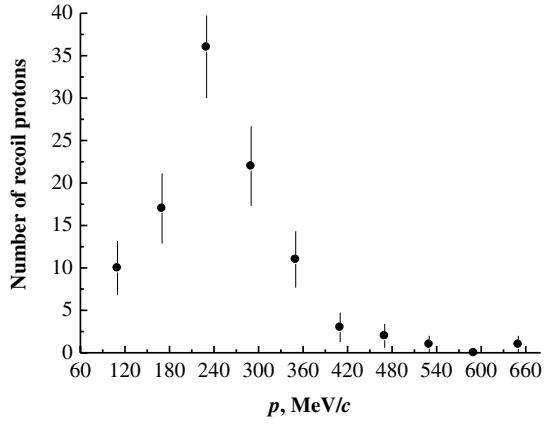

Fig. 2. The momentum distribution of recoil protons with emission angle $\theta \geq 70^\circ$ for reaction in (1) in laboratory frame.

and abruptly descends up to momentum values $p \approx 380\,\mathrm{MeV}/c$, and further the spectrum continues until momenta $p \approx 680\,\mathrm{MeV}/c$. Seemingly the events with recoil protons having momenta $p \leq 380\,\mathrm{MeV}/c$ and emission angles $\theta \geq 70^\circ$ can be considered as candidate events of diffractive breakup of oxygen nucleus.

To find out how such breakup occurs, we considered the events in reaction (1) with recoil protons having emission angles $\theta \geq 70^\circ$ and momenta $p \leq 380\,\mathrm{MeV}/c$. After such constraints on emission angle and momentum of recoil protons, there remained 96 collision events corresponding to cross-section of $4.13 \pm 0.42\,\mathrm{mb}$.

Transverse momentum distribution of recoil protons and spectrum of invariant masses of a pair of ^{12}C and ^{4}He nuclei in these selected events are presented in Fig. 3. As seen from Fig. 3(a), spectrum of transverse momentum of recoil protons has a similar shape as that of total momentum of such protons (see Fig. 2), which is obviously due to their large ($\theta \geq 70^\circ$) emission angles. The mean value and width of transverse momentum distribution of recoil protons in Fig. 3(a) proved to be ≈ 230 and $\approx 60\,\mathrm{MeV}/c$, respectively. The scaled invariant mass distribution of a pair of ^{12}C and ^{4}He nuclei on $\Delta M = M_{\mathrm{inv}}(^{12}\mathrm{C}\alpha)$-$M(^{12}\mathrm{C})$-M($\alpha$) in Fig. 3(b) is characterized by a narrow peak near minimal values of $\Delta M(\sim 5\,\mathrm{MeV}/c^2)$. Furthermore, the spectrum on ΔM decreases approximately exponentially in region $\Delta M > 15\,\mathrm{MeV}/c^2$.

As seen from Fig. 4, the spectrum on difference of azimuthal angles of recoil proton and α particle in the analyzed events is isotropic in region $\Delta\varphi_{\mathrm{p}\alpha} < 108^\circ$, and starting from $\Delta\varphi_{\mathrm{p}\alpha} \geq 108^\circ$ its rise is observed, reaching the maximum value at $\Delta\varphi_{\mathrm{p}\alpha} \approx 170^\circ$. Since the number of final particles is equal to three, the shape of this spectrum should be approximately isotropic, if an oxygen nucleus gets excited as a whole, i.e., if it interacts with a target proton as the one whole unit. It is seen from spectrum on $\Delta\varphi_{p\alpha}$ that the main fraction of events proceeds through direct

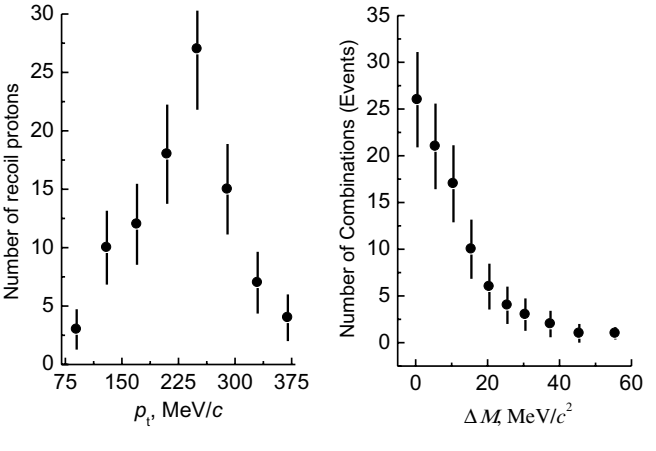

(a) (b)

Fig. 3. (a) Transverse momentum distribution of recoil protons and (b) spectrum on $\Delta M = M_{\mathrm{inv}}(^{12}\mathrm{C}\alpha)$-$M(^{12}\mathrm{C})$-M($\alpha$) of a pair of ^{12}C and ^{4}He nuclei.

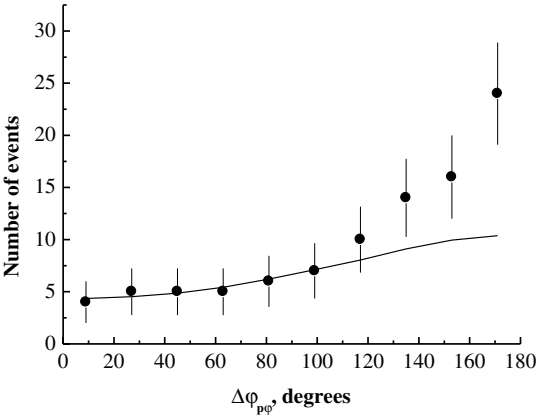

Fig. 4. Distribution of events on difference of azimuthal angles of recoil proton and α particle: • — experiment, solid curve — MC calculations in framework of isotropic phase space model, normalized in region $\Delta\varphi_{p\alpha} \leq 108^{\circ}$.

breakup of an oxygen nucleus on α particle and ^{12}C nucleus, and the remaining part is due to mechanism of quasi elastic knocking out of one of the oxygen α clusters by a proton target.

To determine the contributions of these mechanisms to the channel of oxygen breakup on α particle and ^{12}C nucleus with conservation of recoil proton in final state, we calculated the spectrum on difference of azimuthal angles of recoil proton and α particle within the framework of phenomenological Monte Carlo (MC) model of isotropic phase space.

The aim of MC calculations is to check a hypothesis that, as a result of diffractive interaction of impinging ^{16}O nucleus with the target proton at rest, the oxygen nucleus gets excited as the whole and breaks up isotropically (in its rest frame) into ^{4}He and ^{12} nuclei in their ground state:

$$^{16}\mathrm{O} + p \rightarrow {}^{16}\mathrm{O}* + p' \rightarrow {}^{4}\mathrm{He} + {}^{12}\mathrm{C} + p'. \tag{2}$$

The projections of momenta of recoil proton p' and ^{4}He and ^{12}C nuclei were measured in 96 analyzed experimental events. Therefore, knowing the momentum of impinging ^{16}O nucleus, we can reconstruct the invariant mass of the excited oxygen nucleus, Lorentz parameter and rotation angles, relating the center-of-mass system (CMS) K$'$ of the excited oxygen nucleus and laboratory frame K, in which an incident ^{16}O nucleus impinges along z-axis on proton at rest.

We can generate 1000 times an isotropic breakup of excited ^{16}O* nucleus on two ^{4}He and ^{12}C nuclei for each of 96 experimental events, and then transform their energies and momentum projections into laboratory frame, where we can compare the calculated angular characteristics with the corresponding characteristics of particles in experiment. Then the deviation of experimental spectrum from calculated distribution will point out the existence of anisotropic processes (for

example, knocking out of some nuclear structure (cluster) of oxygen nucleus by a proton target).

In laboratory system K, the energy, momentum projections, and invariant mass of excited oxygen nucleus were determined using the following formulas:

$$\begin{aligned} E_{^{16}\mathrm{O}^*} &= E_{^4\mathrm{He}} + E_{^{12}\mathrm{C}}, \\ P^x_{^{16}\mathrm{O}^*} &= P^x_{^4\mathrm{He}} + P^x_{^{12}\mathrm{C}}, \quad P^y_{^{16}\mathrm{O}^*} = P^y_{^4\mathrm{He}} + P^y_{^{12}\mathrm{C}}, \quad P^z_{^{16}\mathrm{O}^*} = P^z_{^4\mathrm{He}} + P^z_{^{12}\mathrm{C}}, \text{ and} \\ M_{^{16}\mathrm{O}^*} &= \sqrt{(E_{^{16}\mathrm{O}^*})^2 - (P^x_{^{16}\mathrm{O}^*})^2 - (P^y_{^{16}\mathrm{O}^*})^2 - (P^z_{^{16}\mathrm{O}^*})^2}, \end{aligned} \tag{3}$$

where $E_{^4\mathrm{He}}, E_{^{12}\mathrm{C}}$ are experimental energies, and $P^{x,y,z}_{^4\mathrm{He}}, P^{x,y,z}_{^{12}\mathrm{C}}$ are projections of momenta of ^{4}He and ^{12}C nuclei in laboratory frame K.

For transformation from laboratory frame K to CMS K$'$ of the excited oxygen nucleus, we have to turn z-axis in laboratory frame along the momentum vector $\mathbf{P}_{^{16}\mathrm{O}^*}$ of the excited oxygen nucleus. We obtain a new axis z^* of a new system K*, where we choose an axis y^* along the direction of a vector product $\mathbf{z}^* \times \mathbf{z}$. Let the system K* move with a velocity $\boldsymbol{\beta} = \mathbf{P}_{^{16}\mathrm{O}^*}/E_{^{16}\mathrm{O}^*}$ and Lorentz factor $\gamma = 1/\sqrt{1-\beta^2}$. In this way, we obtain the system K$'$ of rest of the excited oxygen nucleus with mass $M_{^{16}\mathrm{O}^*}$ (see reaction in (2)).

In this system K$'$, we generated isotropic decay of the excited oxygen nucleus ^{16}O* on ^{4}He and ^{12}C nuclei. Using random numbers r_1 and r_2, the polar ϕ' and azimuthal θ' angles were generated according to relations

$$\varphi' = 2\pi r_1, \quad \text{and} \quad \mathrm{Cos}\ \theta_{\prime} = 2r_2 - 1 \tag{4}$$

and the energy and modulus of momentum of ^{12}C nucleus were defined using the formulas

$$\begin{aligned} E_{^{12}\mathrm{C}} &= (M^2_{^{16}\mathrm{O}^*} + M^2_{^{12}\mathrm{C}} - M^2_{^4\mathrm{He}})/(2M_{^{16}\mathrm{O}^*}), \\ P_{^{12}\mathrm{C}} &= \sqrt{(E_{^{12}\mathrm{C}})^2 - (M_{^{12}\mathrm{C}})^2}. \end{aligned} \tag{5}$$

Then, in system K$'$, using formulas in (4) and (5), the momentum components of ^{12}C nucleus were determined. The energy and momentum components of ^{4}He nucleus in system K$'$ of rest of ^{16}O* nucleus were defined from the law of energy–momentum conservation.

For Lorentz transformation of the longitudinal components of momenta and energies of ^{4}He and ^{12}C nuclei from system K$'$ to system K*, we used the above obtained values of β and γ.

The so obtained components of MC momentum of ^{12}C nucleus were transformed from system K* to system K using formulas[12]:

$$\begin{aligned} \left(p^{\mathrm{MC}}_{^{12}\mathrm{C}}\right)_x &= -\left(p_{^{12}\mathrm{C}}\right)^*_x \cos\theta\cos\varphi - \left(p_{^{12}\mathrm{C}}\right)^*_y \sin\varphi - \left(p_{^{12}\mathrm{C}}\right)^*_z \sin\theta\cos\varphi, \\ \left(p^{\mathrm{MC}}_{^{12}\mathrm{C}}\right)_y &= -\left(p_{^{12}\mathrm{C}}\right)^*_x \cos\theta\sin\varphi + \left(p_{^{12}\mathrm{C}}\right)^*_y \cos\varphi - \left(p_{^{12}\mathrm{C}}\right)^*_z \sin\theta\sin\varphi, \\ \left(p^{\mathrm{MC}}_{^{12}\mathrm{C}}\right)_z &= -\left(p_{^{12}\mathrm{C}}\right)^*_x \sin\theta - \left(p_{^{12}\mathrm{C}}\right)^*_z \cos\theta, \end{aligned}$$

where (see formulas in (3))

$$\cos\theta = -P^z_{^{16}\mathrm{O}^*}\Big/\sqrt{\left(P^x_{^{16}\mathrm{O}^*}\right)^2+\left(P^y_{^{16}\mathrm{O}^*}\right)^2+\left(P^z_{^{16}\mathrm{O}^*}\right)^2},$$

$$\sin\theta = \left(1-\left(\cos\theta\right)^2\right)^{0.5},$$

$$\cos\varphi = -P^x_{^{16}\mathrm{O}^*}\Big/\sqrt{\left(P^x_{^{16}\mathrm{O}^*}\right)^2+\left(P^y_{^{16}\mathrm{O}^*}\right)^2},$$

$$\sin\varphi = -P^y_{^{16}\mathrm{O}^*}\Big/\sqrt{\left(P^x_{^{16}\mathrm{O}^*}\right)^2+\left(P^y_{^{16}\mathrm{O}^*}\right)^2}.$$

Analogous transformations were made for components of MC momentum of ^{4}He nucleus.

For each generated event, the following quantity was being calculated in laboratory system K:

$$\begin{aligned}\psi = {} & ([(P^{\mathrm{exp}}_{^{12}\mathrm{C}})_x + (P^{\mathrm{exp}}_{^4\mathrm{He}})_x - (p^{\mathrm{MC}}_{^{12}\mathrm{C}})_x - (p^{\mathrm{MC}}_{^4\mathrm{He}})_x]^2/[(P^{\mathrm{exp}}_{^{12}\mathrm{C}})_x + (P^{\mathrm{exp}}_{^4\mathrm{He}})_x]^2 \\ & + [(P^{\mathrm{exp}}_{^{12}\mathrm{C}})_y + (P^{\mathrm{exp}}_{^4\mathrm{He}})_y - (p^{\mathrm{MC}}_{^{12}\mathrm{C}})_y - (p^{\mathrm{MC}}_{^4\mathrm{He}})_y]^2/[(P^{\mathrm{exp}}_{^{12}\mathrm{C}})_y + (P^{\mathrm{exp}}_{^4\mathrm{He}})_y]^2 \\ & + [(P^{\mathrm{exp}}_{^{12}\mathrm{C}})_z + (P^{\mathrm{exp}}_{^4\mathrm{He}})_z - (p^{\mathrm{MC}}_{^{12}\mathrm{C}})_z - (p^{\mathrm{MC}}_{^4\mathrm{He}})_z]^2/[(P^{\mathrm{exp}}_{^{12}\mathrm{C}})_z + (P^{\mathrm{exp}}_{^4\mathrm{He}})_z]^2 \\ & + [E^{\mathrm{exp}}_{^{12}\mathrm{C}} + E^{\mathrm{exp}}_{^4\mathrm{He}} - E^{\mathrm{MC}}_{^{12}\mathrm{C}} - E^{\mathrm{MC}}_{^4\mathrm{He}}]^2/[E^{\mathrm{exp}}_{^{12}\mathrm{C}} + E^{\mathrm{exp}}_{^4\mathrm{He}}]^2)^{0.5}.\end{aligned}$$

A condition $\psi < 10^{-10}$ was being fulfilled for each generated MC event. In this way, the energy–momentum conservation was implemented with the relative precision 10^{-10} at all the stages of event generation.

Distributions of events on difference of azimuthal angles of recoil proton and α particle in experiment and within MC model of isotropic phase space are presented in Fig. 4. MC calculations were normalized in region $\Delta\varphi_{p\alpha} \leq 108^\circ$. In framework of phenomenological model of isotropic phase space, excitation of oxygen nucleus occurs in its peripheral interaction with proton target, and breakup of oxygen nucleus in its rest frame is isotropic. Thus this model allows one to determine, from experimental spectrum on $\Delta\varphi_{p\alpha}$, the fraction of collision events pertaining to diffractive breakup of oxygen nucleus on α particle and ^{12}C nucleus. Then the remaining part of events can be classified as those due to mechanism of quasi elastic knocking out of one of the oxygen α clusters by a proton target.

As seen from Fig. 4, MC calculations describe quite satisfactorily the experimental spectrum in region $\Delta\varphi_{p\alpha} \leq 108^\circ$. The corresponding number of events falling under the calculated spectrum proved to be 70 ± 8 corresponding to cross-section 3.01 ± 0.36 mb, and these events can be taken as those due to diffractive breakup of oxygen nucleus on α particle and ^{12}C nucleus. An excess of the number of experimental events over the calculated spectrum in region $\Delta\varphi_{p\alpha} \geq 108^\circ$ proved to be 26 ± 5 corresponding to cross-section 1.12 ± 0.12 mb, and these events can be classified as those due to mechanism of quasi elastic knocking out of one of the oxygen α clusters by a proton target.

3. Summary and Conclusions

The detailed analysis of channels of breakup of oxygen nucleus on fragments with charges two and six in interactions with protons at 3.25 GeV/c per nucleon was conducted. The experimental mean multiplicities of proton fragments, charged pions, and recoil protons were determined in these channels of oxygen breakup. The mean multiplicities of proton fragments coincided within statistical uncertainties with those of both positive pions and negative pions in topology (26). It was observed that recoil proton was retained in more than 80% of experimental events in this topology. In more than half of the experimental events of oxygen breakup on fragments with charges two and six, the joint formation of α particle and ^{12}C nucleus was observed. Experimental spectrum on difference of azimuthal angles of α particle and recoil proton in reaction $^{16}\mathrm{O} + p \to {}^{4}\mathrm{He} + {}^{12}\mathrm{C} + p$ was compared with the calculations in framework of MC model of isotropic phase space. Based on this comparison, the contributions of mechanism of diffractive breakup of oxygen nucleus and mechanism of quasi elastic knocking out of one of the α clusters of oxygen nucleus by a target proton were determined, which proved to be 3.01 ± 0.36 mb and 1.12 ± 0.12 mb, respectively.

References

1. P. I. Zarubin, Tomography of the cluster structure of light nuclei via relativistic dissociation, in *Clusters in Nuclei*, Vol. 3, ed. C. Beck, Vol. 875 of the series *Lecture Notes in Physics* (Springer International Publisher, Switzerland, 2014), pp. 51–93.
2. N. P. Andreeva *et al.*, *Eur. Phys. J. A* **27** (2006) 295.
3. D. A. Artemenkov *et al.*, *Phys. At. Nucl.* **70** (2007) 1222.
4. T. V. Shedrina *et al.*, *Phys. At. Nucl.* **70** (2007) 1230.
5. M. Karabova *et al.*, *Phys. At. Nucl.* **72** (2009) 300.
6. P. I. Zarubin, *JINR Communications* P1-2010-75, Dubna (2010).
7. K. Olimov *et al.*, *Int. J. Mod. Phys. E* **23** (2014) 1450086.
8. K. N. Abdullaeva *et al.*, *Rep. Uzbek Acad. Sci.* **5** (1996) 21.
9. V. V. Glagolev *et al.*, *Rep. Uzbek Acad. Sci.* **12** (1999) 16.
10. V. V. Glagolev *et al.*, *Eur. Phys. J A* **11** (2001) 285.
11. Kh. K. Olimov, *Phys. At. Nucl.* **71** (2008) 405.
12. V. M. Chudakov and V. V. Lugovoi, *Z. Phys. C* **59** (1993) 511.